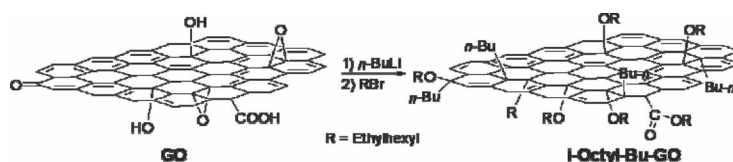


# Functionalization of Graphene Oxide by Two-Step Alkylation

Yi Huang, Weibo Yan, Yanfei Xu, Lu Huang, Yongsheng Chen\*

A new reaction sequence for the chemical functionalization of graphene oxide (GO) consisting of the nucleophilic addition of *n*-butyllithium (*n*-BuLi) to the GO sheets and a subsequent coupling and etherification reaction of the intermediates (Bu-GO)<sup>*n*-Li<sup>n+</sup></sup> and 2-ethylhexyl bromide leading to functionalized GO is developed. The reaction is investigated. The results show that the *n*-Bu and 2-ethylhexyl are covalently attached to the GO sheets and many sp<sup>3</sup> carbons are formed by addition reaction of *n*-BuLi to the plane of GO. After functionalization, the dispersibility of functionalized GO in ortho-dichlorobenzene (ODCB) increases significantly to 0.4 mg mL<sup>-1</sup> and the structural integrity of the graphene sheets remained. Good electronic conductivity of the film prepared from functionalized GO (i-Octyl-Bu-GO) in ODCB is obtained after high temperature annealing.



## 1. Introduction

Graphene, with an atomically thin, 2D structure that consists of sp<sup>2</sup>-hybridized carbons, has attracted enormous interest in the area of solid-state electronics<sup>[1–4]</sup> and composite materials<sup>[5–16]</sup> because of its fascinating electronic and mechanical properties. To further broaden the scope of applications, such as graphene-based organic and polymer composite materials or organic photoelectric device utilizing graphene sheets as active layers,<sup>[17]</sup> and graphene-based chemistry reaction in nonpolar medium,<sup>[18]</sup> new strategies to produce dispersions of graphite oxide (GO) or graphene sheets with good nonpolar organic solution processibility are required. So far, the chemical reduction of exfoliated GO appears to be a more feasible fabrication technique for mass production of reduced graphene

sheets.<sup>[19–23]</sup> So, improving dispersion of GO in nonpolar organic solvents was a better way to solve the problems above. Chemical functionalized GO or graphene in nonpolar organic solvents such as ortho-dichlorobenzene (ODCB) has been rarely addressed. Consequently, there is an urgent demand for the development of a facile and efficient approach to produce large-scale processable GO in nonpolar organic solvents.

It has been reported that C<sub>60</sub> and carbon nanotube can react with alkyl lithium, giving alkylated metal fullerides such as RC<sub>60</sub><sup>-Li<sup>+</sup></sup> or (R<sub>*n*</sub>MWNT<sup>*n*-</sup>)Li<sup>*n*+</sup>.<sup>[24–26]</sup> It is well-known that GO contains many defects with epoxide, hydroxyl, carbonyl, and carboxylic acid groups, as well as double bonds on the GO sheets, which are potentially reactive and can be attacked by nucleophiles such as lithium alkyls.<sup>[22,27–29]</sup>

In this work, we report a new method for functionalization of GO, which uses *n*-butyllithium (*n*-BuLi) to attack the GO sheets, following by coupling and etherification reaction with alkyl bromide. We also demonstrate that such chemical treatment dramatically alters the dispersion behavior of GO sheets and allows for the complete dispersion of GO into individual chemically derivatized GO sheets to be achieved in ODCB.

Assoc. Prof. Y. Huang, Dr. W. Yan, Dr. Y. Xu,  
Dr. L. Huang, Prof. Y. Chen

Key Laboratory of Functional Polymer Materials and Center  
for Nanoscale Science & Technology, Institute of Polymer  
Chemistry, College of Chemistry, Nankai University,  
Tianjin 300071, China  
E-mail: yscheng9@nankai.edu.cn

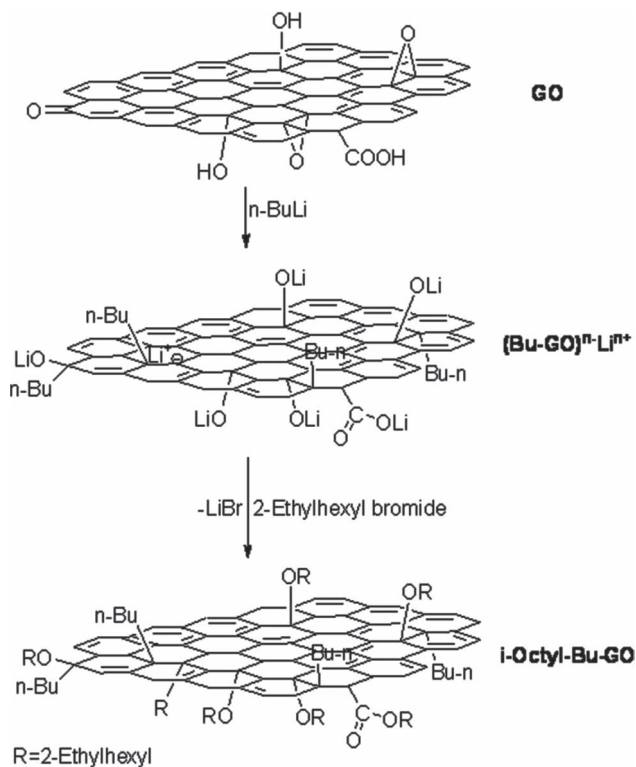


**Figure 1.** Proposed reactions during the treatment of GO with n-BuLi and then with 2-ethylhexyl bromide resulting in the alkyl-functionalized-GO material (i-Octyl-Bu-GO).

## 2. Results and Discussion

The synthesis procedure is shown in Figure 1. GO was prepared according to a modified Hummers method.<sup>[30,31]</sup> The GO was confirmed to exist as single sheets in solution, as AFM image shown in Figure 7A. On the top and bottom of the GO sheets, epoxy and hydroxyl functional groups are present as well as most carbonyl and carboxylic acid groups distributed on the edge. These functional groups and reactive double bonds on the GO sheets could react with n-BuLi. After reaction of n-BuLi and GO sheets, (Bu-GO)<sup>n</sup>-Li<sup>n+</sup> formed, which offer rich nucleophilic centers to react electrophilic reagents such as alkyl bromides to undergo nucleophilic replacement or addition with (Bu-GO)<sup>n</sup>-Li<sup>n+</sup> to generate functionalized graphene materials, i-Octyl-Bu-GO. Then, 2-ethylhexyl bromide was added with precipitation of LiBr, and 2-ethylhexyl-attached onto the GO sheets. Considering complete drying of GO is probably impossible,<sup>[32,33]</sup> so excess of n-BuLi was added. After functionalization, GO could hardly disperse in water and the dispersibility of GO in ODCB increases significantly because of the presence of alkyl chains groups attaching to the GO sheets. The functionalized GO (i-Octyl-Bu-GO) was investigated by FTIR, UV-Vis NIR spectroscopy, Raman spectroscopy, TGA, TEM, AFM.

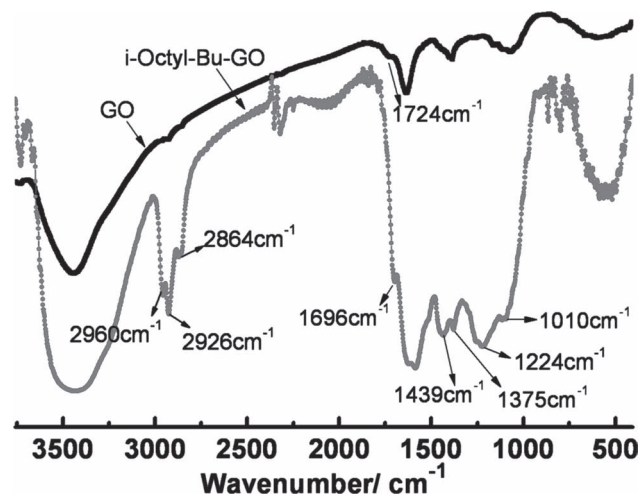
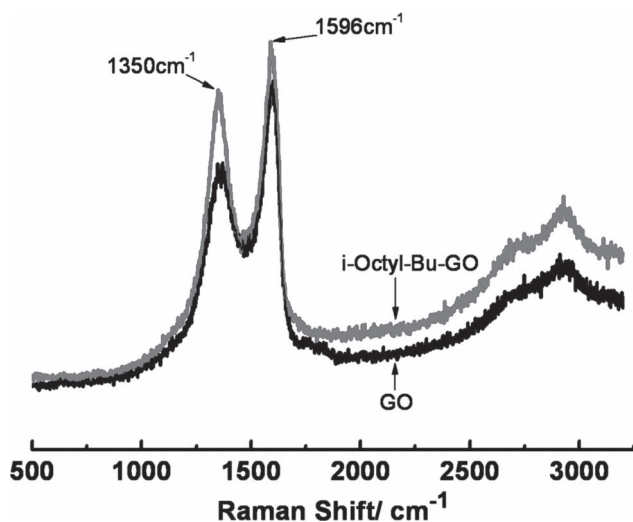


**Figure 2.** FTIR spectra of GO, i-Octyl-Bu-GO. Strong stretching vibration of C—H at 2960, 2926, 2864 cm<sup>-1</sup> in i-Octyl-Bu-GO indicates functional alkyl chain groups are chemically attached to the GO sheets.

Figure 2 shows the FTIR spectra of GO, i-Octyl-Bu-GO. As shown in Figure 2, the intense absorption peaks at 2960, 2926, 2864 cm<sup>-1</sup> are attributed to the stretching vibration of —CH<sub>2</sub>— and —CH<sub>3</sub>. The peaks at 1439, 1375 cm<sup>-1</sup> are attributed to the deformation vibration of —CH<sub>2</sub>— and —CH<sub>3</sub>.<sup>[34]</sup> These confirmed many n-Bu have been chemically attached to the GO sheets. Furthermore, the absorption peak of C—O—H at 1390 cm<sup>-1</sup> in i-Octyl-Bu-GO disappeared, new peaks at 1216 and 1010 cm<sup>-1</sup> corresponding to the O—Ar and O—R (R = 2-ethylhexyl) stretching vibration are clearly observed, which indicates the 2-ethylhexyl bromide reacts with the (Bu-GO)<sup>n</sup>-Li<sup>n+</sup>.<sup>[35]</sup> The stretching vibration of C=O at 1742 is shift to 1696 cm<sup>-1</sup> because the group COOH converted to COOR (R = 2-ethylhexyl) after reaction as shown in Figure 1.<sup>[34]</sup>

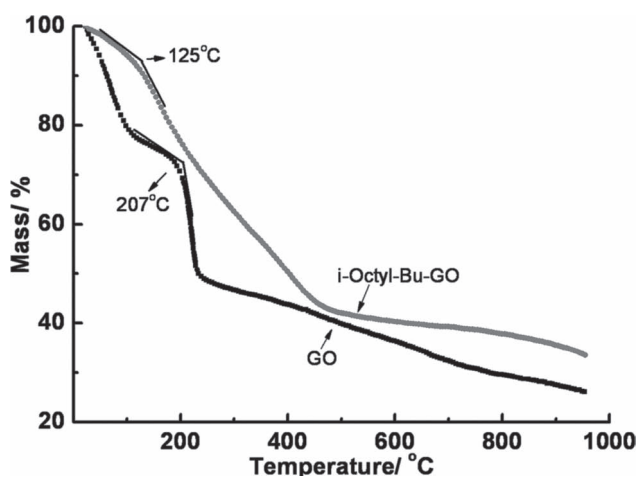
Raman spectroscopy of the GO, i-Octyl-Bu-GO was conducted, as shown in Figure 3. The GO shows an intense tangential mode (G band) at 1596 cm<sup>-1</sup>, with a disordered-induced peak (D band) at 1350 cm<sup>-1</sup>. Comparing with of GO, G and D mode of i-Octyl-Bu-GO is not greatly changed. However, the ratio of the intensities (ID/IG = 0.87) for i-Octyl-Bu-GO samples is markedly increased compared with that (ID/IG = 0.75) of GO, indicating the formation of much sp<sup>3</sup> carbon on the graphene plane, reflecting the increase in disorder after functionalization.<sup>[33,36–38]</sup> These indicate the successful covalent modification of GO by a generic organometallic approach.

Figure 4 shows the TGA curves of the GO and i-Octyl-Bu-GO. GO is thermally unstable and starts to lose mass upon heating even below 100 °C, mainly attributed to the removal of absorbed water. The major mass loss occurs at 207 °C, presumably due to pyrolysis of the labile oxygen-containing functional groups.<sup>[33]</sup> The GO shows a large



**Figure 3.** Raman spectra of GO and i-Octyl-Bu-GO. The ratio of the intensities ( $ID/IG = 0.87$ ) for i-Octyl-Bu-GO is markedly increased compared with that ( $ID/IG = 0.75$ ) of GO, indicating the break of C=C and the formation of much  $sp^3$  carbon in i-Octyl-Bu-GO by the nucleophilic addition of  $n\text{-BuLi}$  to the plane of GO.

weight loss (20%) with an onset temperature at 207 °C. Compared with the curve of GO, the weight loss of i-Octyl-Bu-GO below 240 °C is lower, indicating that the main oxygen-containing functional groups of GO have been converted after functionalization. The maximum mass loss temperature (ca. 360 °C) of i-Octyl-Bu-GO sheets was roughly 150 °C higher than that of GO. After 240 °C, i-Octyl-Bu-GO shows a faster weight loss than GO, which was attributed to the remove of functionalized alkyl chains, until they have almost the same weight loss of



**Figure 4.** TGA curves of GO and i-Octyl-Bu-GO obtained with a heating rate of  $5\text{ °C min}^{-1}$  under purified nitrogen gas flow. Compared with GO, the slower the weight loss of i-Octyl-Bu-GO below 240 °C indicates the main oxygen-containing functional groups of GO have been converted to thermal stability functional groups after generic reaction.

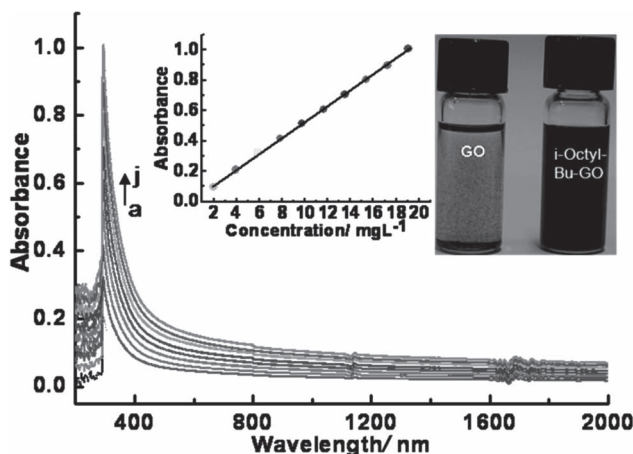


**Figure 5.** Concentration dependence of UV absorption of i-Octyl-Bu-GO in ODCB (concentrations are 1.99, 3.96, 5.91, 7.84, 9.76, 11.65, 13.53, 15.38, 17.22, 19.05  $\text{mg L}^{-1}$  from a to j, respectively). Shown in the inset are a plot of optical density at maximal absorption position (295 nm) for the GO moiety versus concentration and optical image of GO and i-Octyl-Bu-GO dispersed in ODCB ( $0.4\text{ mg mL}^{-1}$ ), respectively.

ca. 60% at 460 °C. These results are similar to  $n$ -butyllium functionalized single-walled carbon nanotubes.<sup>[39]</sup> These results demonstrate that after functionalization, i-Octyl-Bu-GO has better thermal stability than GO.

The prevention of aggregation is of particular importance for processibility and applications of GO or graphene because most of its attractive properties are only associated with individual graphene sheets. Solution-phase UV-Vis-NIR spectroscopy can be used to determine the solubility of i-Octyl-Bu-GO.<sup>[40]</sup> Figure 5 shows the absorption spectra of solutions of i-Octyl-Bu-GO with different concentrations. The absorptions (at 295 nm) for the GO moiety were plotted against concentration (Figure 5 inset) and a good linear relationship was obtained with an  $R$  value of 0.9997.<sup>[21]</sup> Assuming the applicability of Beer's law, from the slope of the linear least-squares fit we estimated the effective extinction coefficient of the i-Octyl-Bu-GO to be  $0.053\text{ L mg}^{-1}\text{ cm}^{-1}$  in ODCB at this position. The absorbance of solutions of i-Octyl-Bu-GO at other wavelengths was also consistent with the Beer's law. The straight line in the plot in the inset is a linear least-squares fit to the data, indicating the hybrid i-Octyl-Bu-GO was dissolved homogeneously in the solvent. These results demonstrate that i-Octyl-Bu-GO has much better solubility than GO in ODCB, which could be obviously demonstrated in an optical image inset of GO and i-Octyl-Bu-GO dispersed in ODCB ( $0.4\text{ mg mL}^{-1}$ ).

In order to further investigate the morphology of GO and i-Octyl-Bu-GO, TEM measurements have also been performed. The resulting GO (in water) and i-Octyl-Bu-GO (in ODCB) dispersions of  $0.1\text{ mg mL}^{-1}$  were placed directly on Cu grids and examined under a TEM. The materials

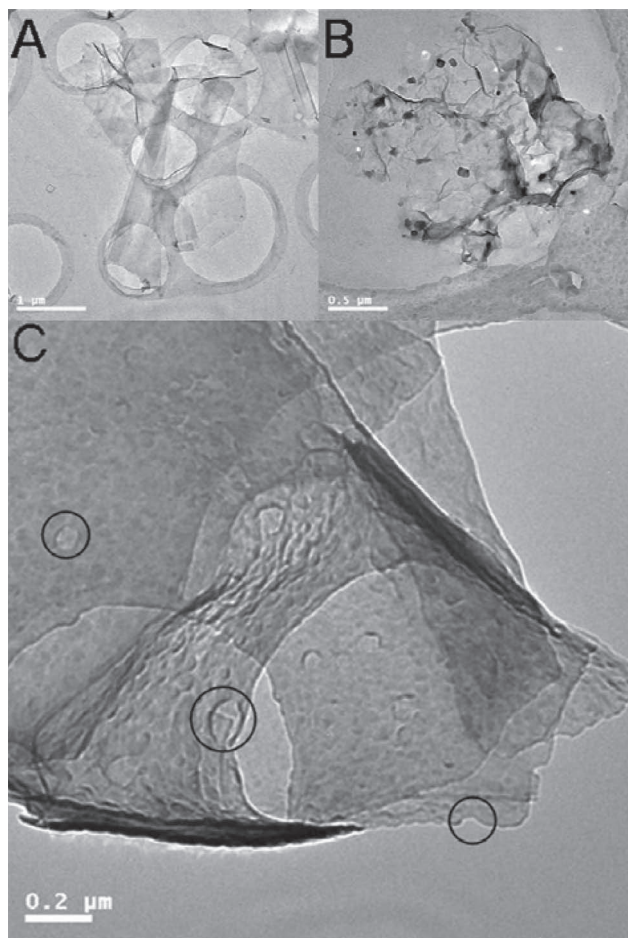


**Figure 6.** A) TEM images of GO, B, C) TEM images i-Octyl-Bu-GO. Functionalized sample i-Octyl-Bu-GO is still monolayer dispersion but the surface becomes coarser with many defects after functionalization.

of GO sheets that we used in the reaction monolayer dispersed and was smooth and transparent, as shown in Figure 6A. The TEM images of i-Octyl-Bu-GO (Figure 6B and C) show that mostly functionalized GO are single layers i-Octyl-Bu-GO.

In Figure 6B, part of small flakes on functionalized GO (i-Octyl-Bu-GO) was wrinkled, probably induced by the reaction and electron beam when the sample was tested. As Figure 6C shown, after functionalization, the surface of the GO became much coarser with many visible defects (marked with circle), which was attributed to vigorous oxidation reaction in the preparation of GO and the energetic reaction between GO and n-BuLi. Distortions caused by the functional groups and the extremely small thickness of the resulting i-Octyl-Bu-GO sheets lead to a wrinkled topology. Despite all this, as Figure 6B shows, large graphitic domains are visible and the single layer of GO still retained structural integrity of the graphene framework. The morphology and well dispersion of the i-Octyl-Bu-GO

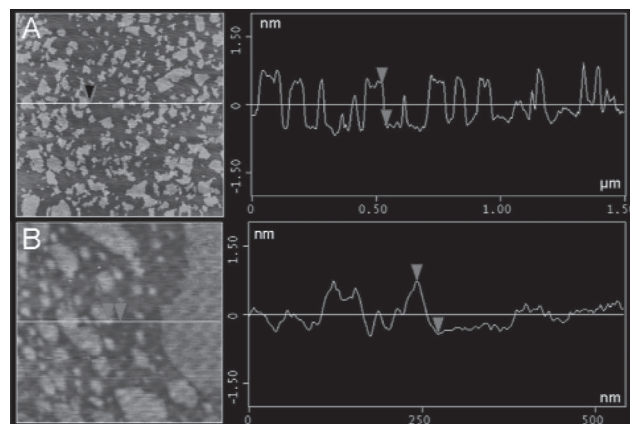


**Figure 7.** A) AFM image of GO sheets on a mica surface. B) AFM image of i-Octyl-Bu-GO sheets on a mica surface. Single sheets of i-Octyl-Bu-GO with an average thickness of about 0.8 nm are present, with different lateral dimensions between 20 and 200 nm.

sheets obtained in this work, which is very important for further preparation of nanocomposite materials based on GO or graphene.

We employed AFM to establish the thickness and surface roughness of the depositions. The samples were prepared by depositing well-dispersed GO in H<sub>2</sub>O (0.1 mg mL<sup>-1</sup>) and i-Octyl-Bu-GO in ODCB (0.1 mg mL<sup>-1</sup>) on new cleaved mica surfaces and drying in air. AFM images of i-Octyl-Bu-GO in Figure 7B show the areas in which single sheets with a thickness of about 0.8 nm are present, and with different lateral dimensions between 20 and 200 nm.

Compared with images of GO shown in Figure 7A, The size and thickness of GO sheets have no obvious change, which is consistent with a single layer of functionalized GO or graphene.<sup>[41,42]</sup> Although many alkyl chains attached to the surface or edge but were relatively short and flexible, it have little effect on the thickness of GO sheets.

The electrical conductivity of the as-prepared alkyl-modified-graphene oxide and thermally reduced alkyl-modified-graphene oxide film were measured at room temperature. At a given film thickness of ca. 100 nm, concomitant increase of film conductivity was observed with an increase in the heating temperatures from 300 to 1000 °C. As shown in Table 1, the conductivity of film for i-Octyl-Bu-GO increases with temperature ascending, which is attributed the content of graphite structure recovered. Because of after functionalization, i-Octyl-Bu-GO becomes thermally more stable than GO, and functional groups were hardly removed by thermal reduction at 300 and 600 °C. However, at 1000 °C, nearly all the functional groups on the GO are removed, the conjugated sp<sup>2</sup> network is largely restored. And due to the thermal fusion and surface-mediated reaction of graphene, it is reasonable to assume that the thermal annealing of the

**Table 1.** Comparison of the dependence of sheet resistance and film ( $\approx 100$  nm thickness) and conductivity of i-Octyl-Bu-GO for different reducing methods.

Graphene films	Sheet resistance [ $\Omega \text{ sq}^{-1}$ ]	Film conductivity [ $\text{S cm}^{-1}$ ]
Hydrazine+300 °C	$8.47 \times 10^{10}$	$1.18 \times 10^{-11}$
Hydrazine+600 °C	$2.88 \times 10^6$	$2.28 \times 10^{-2}$
Hydrazine+1000 °C	$1.88 \times 10^2$	$5.62 \times 10^2$

composite films consisting of graphene sheets and alkyl chains could heal the defects formed by oxide, so it shows high conductivity  $562 \text{ S cm}^{-1}$ , which is consistent with results reported.<sup>[31,43]</sup>

### 3. Conclusion

We have developed a new reaction sequence for the chemical functionalization of GO. The results from FTIR, TGA, Raman clearly indicated that the reaction between n-BuLi and GO occurred successfully. The UV-Vis-NIR, AFM, and TEM images show functionalized chemically converted graphene flakes dispersed as single layer with crumpled silk waves have been obtained in this work, while retaining structural integrity of the graphene framework. The alkyl chains on the GO surface help keep the GO sheets separate and results in the formation of a black homogeneous dispersion of the GO in ODCB. And we also obtain good electronic conductivity of the film prepared from functionalized GO in ODCB after high temperature annealing, which would offer a good substitute for the film prepared from aqueous solution, which would be used as electrode material.

### Supporting Information

Supporting Information is available from the Wiley Online Library or from the author.

**Acknowledgements:** The authors gratefully acknowledge financial support from MOST (Grants 2012CB933401 and 2011DFB50300) and NSFC (Grants 50933003, 50902073 and 50903044).

Received: November 29, 2011; Revised: January 11, 2012;  
Published online: April 17, 2012; DOI: 10.1002/macp.201100658

**Keywords:** conductivity; dispersion; functionalization; graphene oxide; nucleophiles

- [1] K. S. Novoselov, A. K. Geim, S. V. Morozov, D. Jiang, Y. Zhang, S. V. Dubonos, I. V. Grigorieva, A. A. Firsov, *Science* **2004**, *306*, 666.

- [2] Y. B. Zhang, J. W. Tan, H. L. Stormer, P. Kim, *Nature* **2005**, *438*, 201.
- [3] A. K. Geim, K. S. Novoselov, *Nat. Mater.* **2007**, *6*, 183.
- [4] X. L. Li, X. R. Wang, L. Zhang, S. Lee, H. J. Dai, *Science* **2008**, *319*, 1229.
- [5] S. Stankovich, D. A. Dikin, G. H. B. Dommett, K. M. Kohlhaas, E. J. Zimney, E. A. Stach, R. D. Piner, S. T. Nguyen, R. S. Ruoff, *Nature* **2006**, *442*, 282.
- [6] S. Watcharotone, D. A. Dikin, S. Stankovich, R. Piner, I. Jung, G. H. B. Dommett, G. Evmenenko, S. E. Wu, S. F. Chen, C. P. Liu, S. T. Nguyen, R. S. Ruoff, *Nano Lett.* **2007**, *7*, 1888.
- [7] T. Ramanathan, A. A. Abdala, S. Stankovich, D. A. Dikin, M. Herrera-Alonso, R. D. Piner, D. H. Adamson, H. C. Schniepp, X. Chen, R. S. Ruoff, S. T. Nguyen, I. A. Aksay, R. K. Prud'homme, L. C. Brinson, *Nat. Nanotechnol.* **2008**, *3*, 327.
- [8] H. J. Jiang, *Small* **2011**, *7*, 2413.
- [9] X. Huang, Z. Y. Yin, S. X. Wu, X. Y. Qi, Q. Y. He, Q. C. Zhang, Q. Y. Yan, F. Boey, H. Zhang, *Small* **2011**, *7*, 1876.
- [10] X. Huang, X. Y. Qi, F. Boey, H. Zhang, *Chem. Soc. Rev.* **2012**, *41*, 666.
- [11] X. Huang, S. Z. Li, Y. Z. Huang, S. X. Wu, X. Z. Zhou, S. Z. Li, C. L. Gan, F. Boey, C. A. Mirkin, H. Zhang, *Nat. Commun.* **2011**, *2*, 292.
- [12] X. Huang, X. Z. Zhou, S. X. Wu, Y. Y. Wei, X. Y. Qi, J. Zhang, F. Boey, H. Zhang, *Small* **2010**, *6*, 513.
- [13] X. Y. Qi, K.-Y. Pu, H. Li, X. Z. Zhou, S. X. Wu, Q.-L. Fan, B. Liu, F. Boey, W. Huang, H. Zhang, *Angew. Chem. Int. Ed.* **2010**, *49*, 9426.
- [14] X. Y. Qi, K.-Y. Pu, X. Z. Zhou, H. Li, B. Liu, F. Boey, W. Huang, H. Zhang, *Small* **2010**, *6*, 663.
- [15] X. H. Cao, Q. Y. He, W. H. Shi, B. Li, Z. Y. Zeng, Y. M. Shi, Q. Y. Yan, H. Zhang, *Small* **2011**, *7*, 1199.
- [16] X. Huang, H. Li, S. Z. Li, S. X. Wu, F. Boey, J. Ma, H. Zhang, *Angew. Chem. Int. Ed.* **2011**, *50*, 12245.
- [17] Z. F. Liu, Q. Liu, X. Y. Zhang, Y. Huang, Y. F. Ma, S. G. Yin, Y. S. Chen, *Adv. Mater.* **2008**, *20*, 3924.
- [18] C. E. Hamilton, J. R. Lomeda, Z. Z. Sun, J. M. Tour, A. R. Barron, *Nano Lett.* **2009**, *9*, 3460.
- [19] S. Gilje, S. Han, M. S. Wang, K. L. Wang, R. B. Kaner, *Nano Lett.* **2007**, *7*, 3394.
- [20] X. Wang, L. J. Zhi, K. Müllen, *Nano Lett.* **2008**, *8*, 323.
- [21] D. Li, M. B. Müller, S. Gilje, R. B. Kaner, G. G. Wallace, *Nat. Nanotechnol.* **2008**, *3*, 101.
- [22] D. R. Dreyer, S. Park, C. W. Bielawski, R. S. Ruoff, *Chem. Soc. Rev.* **2010**, *39*, 228.
- [23] X. Z. Zhou, X. Huang, X. Y. Qi, S. X. Wu, C. Xue, F. Y. C. Boey, Q. Y. Yan, P. Chen, H. Zhang, *J. Phys. Chem. C* **2009**, *113*, 10842.
- [24] G. Viswanathan, N. Chakrapani, H. Yang, B. Q. Wei, H. Chung, K. Cho, C. Y. Ryu, P. M. Ajayan, *J. Am. Chem. Soc.* **2003**, *125*, 9258.
- [25] R. Graupner, J. Abraham, D. Wunderlich, A. Vencelová, P. Lauffer, J. Röhl, M. Hundhausen, L. Ley, A. Hirsch, *J. Am. Chem. Soc.* **2006**, *128*, 6683.
- [26] A. Hirsch, A. Soi, H. R. Karfunhel, *Angew. Chem. Int. Ed. Engl.* **1992**, *31*, 766.
- [27] S. Park, R. S. Ruoff, *Nat. Nanotechnol.* **2009**, *4*, 217.
- [28] H. Gilman, F. W. Moore, O. Baine, *Interconversion Reactions Alkylolithium Compd.* **1941**, *63*, 2479.
- [29] Y. Maeda, T. Kato, T. Hasegawa, M. Kako, T. Akasaka, J. Lu, S. Nagase, *Org. Lett.* **2010**, *12*, 996.
- [30] W. S. Hummers Jr., R. E. Offeman, *J. Am. Chem. Soc.* **1958**, *80*, 1339.

- [31] H. A. Becerril, J. Mao, Z. F. Liu, R. M. Stoltenberg, Z. N. Bao, Y. S. Chen, *ACS Nano* **2008**, *2*, 463.
- [32] T. Szabó, O. Berkesi, I. Dékány, *Carbon* **2005**, *43*, 3186.
- [33] S. Stankovich, D. A. Dikin, R. D. Piner, K. A. Kohlhaas, A. Kleinhammes, Y. Y. Jia, Y. Wu, S. T. Nguyen, R. S. Ruoff, *Carbon* **2007**, *45*, 1558.
- [34] S. Niyogi, E. Bekyarova, M. E. Itkis, J. L. McWilliams, M. A. Hamon, R. C. Haddon, *J. Am. Chem. Soc.* **2006**, *128*, 7720.
- [35] Y. Y. Liang, D. Q. Wu, X. L. Feng, K. Müllen, *Adv. Mater.* **2009**, *21*, 1679.
- [36] D. Graf, F. Molitor, K. Ensslin, C. Stampfer, A. Jungen, C. Hierold, L. Wirtz, *Nano Lett.* **2007**, *7*, 238.
- [37] I. Calizo, A. A. Balandin, W. Bao, F. Miao, C. N. Lau, *Nano Lett.* **2007**, *7*, 2645.
- [38] K. N. Kudin, B. Ozbas, H. C. Schniepp, R. K. Prud'homme, I. A. Aksay, R. Car, *Nano Lett.* **2008**, *8*, 36.
- [39] D. Wunderlich, F. Hauke, A. Hirsch, *Chem. Eur. J.* **2008**, *14*, 1607.
- [40] Z. Guo, F. Du, D. M. Ren, Y. S. Chen, J. Y. Zheng, Z. B. Liu, J. G. Tian, *J. Mater. Chem.* **2006**, *16*, 3021.
- [41] S. Stankovich, R. D. Piner, S. T. Nguyen, R. S. Ruoff, *Carbon* **2006**, *44*, 3342.
- [42] R. Salvio, S. Krabbenborg, W. J. M. Naber, A. H. Velders, D. N. Reinhoudt, W. G. van der Wiel, *Chem. Eur. J.* **2009**, *15*, 8235.
- [43] Q. Su, S. P. Pang, V. Alijani, C. Li, X. L. Feng, K. Müllen, *Adv. Mater.* **2009**, *21*, 3191.